

## Mylonite fabric development on Naxos, Greece

I. S. BUICK\*

Department of Geology, University of Tasmania, G.P.O. Box 252c, Hobart, Tasmania 7001, Australia

(Received 21 August 1989; accepted in revised form 16 November 1990)

**Abstract**—The Miocene structural evolution of the metamorphic complex on Naxos occurred within a mid- to lower crustal, sub-horizontal shear zone. The deformation style and the regional stress field in the Aegean during the Miocene are consistent with exhumation of the metamorphic complex during ductile crustal thinning. Deformation in this shear zone initiated possibly before, and continued after, the peak of localized high-temperature Barrovian-style metamorphism. Kinematic indicators in non-coaxial fabrics indicate that upper structural levels were displaced to the NNE throughout the Miocene structural history of the metamorphic complex. This displacement was accompanied during its latter stages by compression in an E–W direction.

### INTRODUCTION

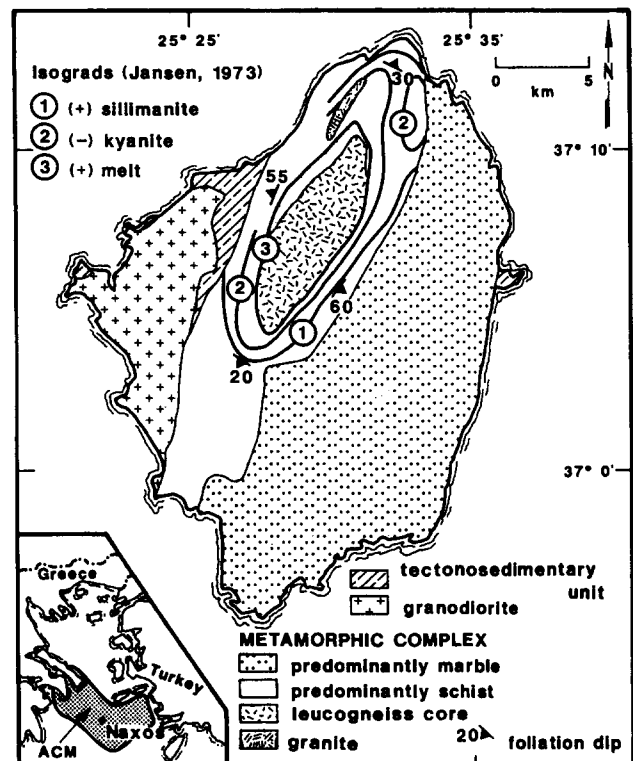
OVER THE past 10–15 years, the role of extensional tectonics in the development of sedimentary basins, at divergent plate boundaries and in the exhumation of regional metamorphic terrains has been widely documented, e.g. McKenzie (1978a,b), Davis & Coney (1979), Davis (1980), Wernicke & Burchfiel (1982), Davis (1987). In particular, theoretical (England & Thompson 1986, England 1987, Sonder *et al.* 1987) and field-based studies (Coney 1987, Dewey 1988, Sandiford 1989) have led to increased recognition of the role of extensional processes in the thermal evolution of metamorphic belts.

Studies of metamorphic terrains exhumed during Cenozoic extension in the Basin and Range province of North America are at the forefront of controversy with regard to the nature of extension of the middle to lower crust. These 'metamorphic core complexes' typically occur as ductilely deformed metamorphic–plutonic basement domes, separated from an overlying unmetamorphosed, fractured and distended sedimentary carapace by low-angle, normal-sense, brittle tectonic contacts (Davis & Coney 1979, Davis 1987). Similar mylonitized metamorphic complexes occur on islands which together comprise the Attic Cycladic Massif, within the south-central Aegean area (Fig. 1). These metamorphic complexes, which experienced Tertiary polymetamorphism, were rapidly uplifted and exhumed during the Miocene. This uplift was suggested by Lister *et al.* (1984) to have occurred in the footwall of a southerly dipping, low-angle normal-sense shear zone, in a manner analogous to that invoked by some workers for Basin and Range 'metamorphic core complexes'. There is, however, a lack of published information with regard to the timing of metamorphism and deformation in the Attic Cycladic Massif. In this paper, recent investigations of the structural and metamorphic evolution of the island of Naxos, within the Attic Cycladic Massif, are

presented in order to further investigate the nature, orientation and timing of Miocene ductile deformation in the south-central Aegean.

### REGIONAL SETTING

The island of Naxos lies in the middle of the Attic Cycladic Massif (Fig. 1). The arcuate trace of this metamorphic belt follows the trend of a present-day active trench system, marking the site of subduction of the African plate northeastwards beneath the Apulian–Anatolian microplate (Robertson & Dixon 1984), south of the island of Crete. Associated Pliocene to present-



\*Present address: Department of Geology, University of Melbourne, Parkville, Victoria 3052, Australia.

Fig. 1. Simplified geology of Naxos, with  $M_{2B}$  field isograds modified after Jansen (1973). Abbreviation: ACM = Attic Cycladic Massif.

day arc-related volcanism defines a volcanic arc immediately to the south of the Attic Cycladic Massif. The Aegean region has been the site of significant middle Miocene and later extension (Le Pichon & Angelier 1979), and is floored by thinned continental crust. In the south-central Aegean region, greatest Pliocene to recent extension occurred to the south of the present-day volcanic arc, in the Sea of Crete. Attenuated continental crust in this region is 18–20 km thick (Makris 1978).

Metamorphic complexes in the Attic Cycladic Massif occur as structural domes and consist of sedimentary sequences of Mesozoic age (Dürr *et al.* 1978) which were tectonically interleaved and polymetamorphosed during the Tertiary. In addition, on several islands relicts of Hercynian metamorphic basement occur within the deepest levels of these structural domes (e.g. Ios—Henjes-Kunst & Kreuzer 1982; Naxos—Andriessen *et al.* 1987). Throughout the Cyclades, metamorphic complexes preserve evidence of blueschist facies metamorphism ( $M_1$ ) of Eocene age (Andriessen *et al.* 1979, Wijbrans *et al.* 1990). On many islands, the  $M_1$  blueschist facies event appears to have been statically overprinted by an Oligo-Miocene regional greenschist facies event of Barrovian character. This event, termed  $M_{2A}$ , has been dated at  $ca\ 25 \pm 5$  Ma on Naxos (Andriessen *et al.* 1979). However, recent single crystal  $^{40}\text{Ar}$ – $^{39}\text{Ar}$  geochronology indicates that several periods of greenschist facies metamorphism may have occurred in the time interval 30–19 Ma in the Cyclades (Wijbrans *et al.* 1990). Several workers have inferred a  $P$ – $T$  segment of near-isothermal decompression for the  $M_1$ – $M_{2A}$  interval (Jansen & Schuiling 1976, Van der Maar 1981, Schliestedt *et al.* 1987).  $M_2$  metamorphism reached upper amphibolite facies, with associated partial anatexis, in a thermal dome of limited areal extent on the island of Naxos (Jansen & Schuiling 1976). High-temperature metamorphism, termed  $M_{2B}$ , occurred on Naxos in the interval 20–16 Ma, most probably at the older (20–19 Ma) end of this interval (Wijbrans & McDougall 1988, Jansen personal communication 1989). Peak metamorphic conditions during this event have been estimated by Buick & Holland (1989 and unpublished data) and Jansen & Schuiling (1976) as  $(6\text{--}7 \pm 2\ \text{kbar}, 670 \pm 50^\circ\text{C})$ .

The metamorphic complex was intruded along its western margin by a post- $M_2$  granodiorite (Fig. 1) in the interval  $ca\ 13\text{--}11$  Ma (Andriessen *et al.* 1979, Wijbrans 1985). Associated with this intrusion was the development of a narrow contact aureole ( $M_3$  of Jansen & Schuiling 1976). Both the metamorphic complex and granodiorite are tectonically overlain by remnants of a structurally disrupted, unmetamorphosed, allochthonous tectonosedimentary unit of Miocene age which contains Palaeozoic debris (Roessler 1978). The juxtaposition of this unit onto deformed crystalline rocks occurred along a low-angle N-dipping tectonic contact (Jansen 1977). The timing of emplacement of the tectonosedimentary unit is poorly constrained. Glass from pseudotachylites developed near the tectonic contact yields a K–Ar age of  $ca\ 9$  Ma (Andriessen *et al.* 1979).

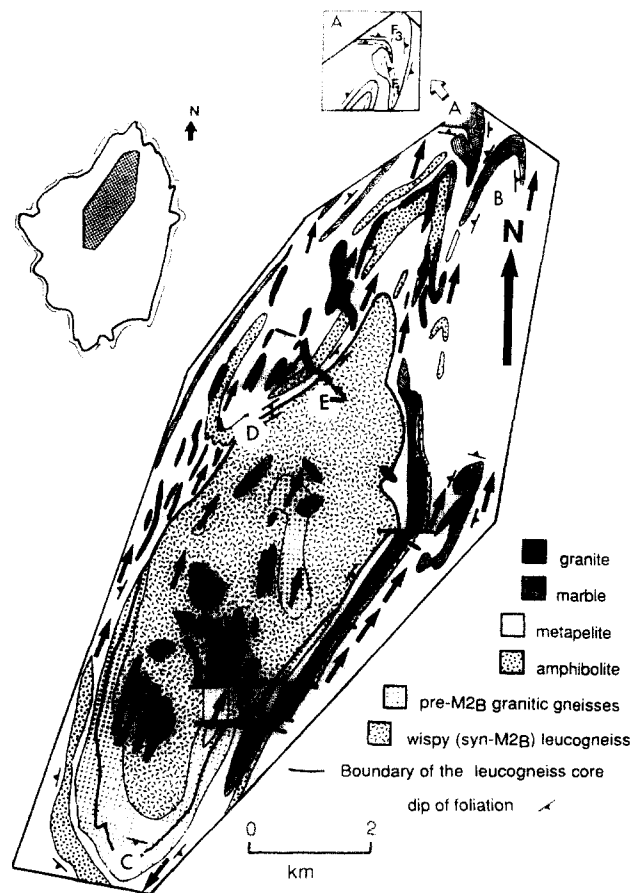


Fig. 2. Geology of the high-grade core of the metamorphic complex. Localities A–E are referred to in the text. Arrows indicate the sense of movement of upper structural levels inferred from kinematic indicators in asymmetric fabrics.

Emplacement of the tectonosedimentary unit on Naxos pre-dates the development of autochthonous conglomerates of Upper Pliocene (i.e. 6–5 Ma) age (Roessler 1978).

## THE STUDY AREA

This paper is concerned with the structural evolution of the high-grade portion of the metamorphic complex (Fig. 2) and the post- $M_2$  granodiorite (Fig. 3). The metamorphic complex predominantly consists of mid- to upper amphibolite facies meta-pelites with subordinate marbles, felsic gneisses and meta-volcanics. It is structurally overlain by greenschist facies marble-dominated sequences (Fig. 1).  $M_{2B}$  isograds (Jansen 1973), originally defined on the basis of index minerals, are oval-shaped and roughly concentric with the structural dome (Fig. 1). More recent study of meta-pelitic assemblages and equilibria (Buick & Holland 1989 and unpublished data) suggests that these are not true isogradic surfaces and that the kyanite-out isograd does not exist. Nevertheless, the distribution of mineral assemblages (Jansen & Schuiling 1976) and quantitative  $P$ – $T$  studies (Buick 1988, Buick & Holland 1989) are consistent with a general increase in  $M_{2B}$  grade towards the core of the structural dome.

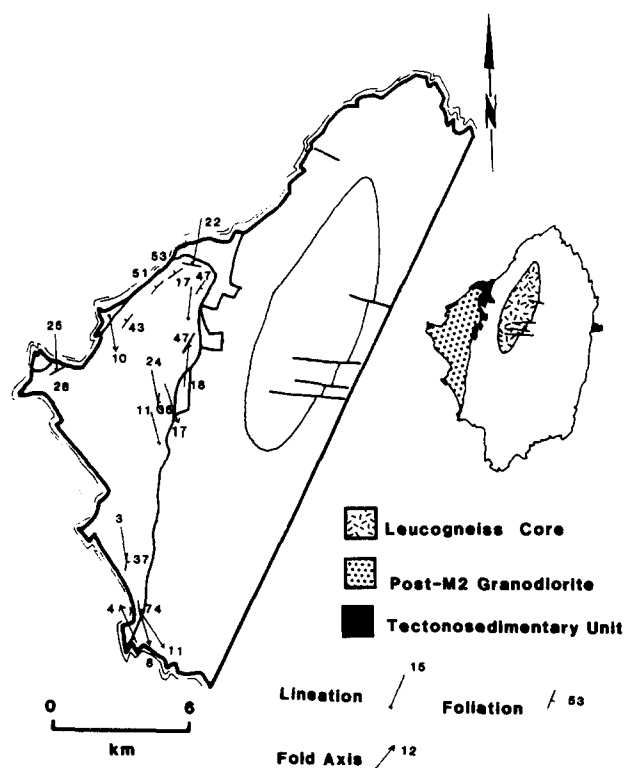


Fig. 3. Geology of the post- $M_2$  granodiorite, showing the orientation of  $S_2$  mylonitic fabrics,  $L_2$  stretching lineations and  $L_3$  crenulation lineations. The distribution of the tectonosedimentary is modified after Jansen (1973).

The meta-pelite-dominated portion of the metamorphic complex is structurally underlain by a core of predominantly migmatitic leucogranitic gneisses, termed the 'leucogneiss core'. Syn- and post- $M_{2B}$  fabrics in the structurally overlying gneisses dip at low to moderate ( $25\text{--}50^\circ$ ) angles away from the leucogneiss core (Fig. 1). The boundary of the leucogneiss core does not correspond exactly to the  $M_{2B}$  melt-in isograd of Jansen & Schuiling (1976). This is because granitic gneisses within the leucogneiss core are of both syn- and pre- $M_{2B}$  origin (Van der Maar & Jansen 1983, Andriessen *et al.* 1987, Buick 1988). These granitic gneisses are interleaved with discontinuous horizons of marble and meta-pelite (Fig. 2).

### STRUCTURAL RELATIONSHIPS IN THE MIDDLE AMPHIBOLITE PORTION OF THE METAMORPHIC COMPLEX

Three generations of mesoscopic folding ( $F_1$ ,  $F_2$  and  $F_3$ ) have been recognized in the high-grade portion of the metamorphic complex. These fold generations have been assigned to three periods of deformation ( $D_1$ ,  $D_2$  and  $D_3$ ), on the basis of overprinting criteria, metamorphic grade, macro- and microstructural fabric development and, to a lesser extent, fold geometry. Fabrics and lineations associated with these deformational events are depicted in stereographic form in Fig. 4. Throughout the remaining text, reference will be made to the transport direction implied by stretching lineations and asym-

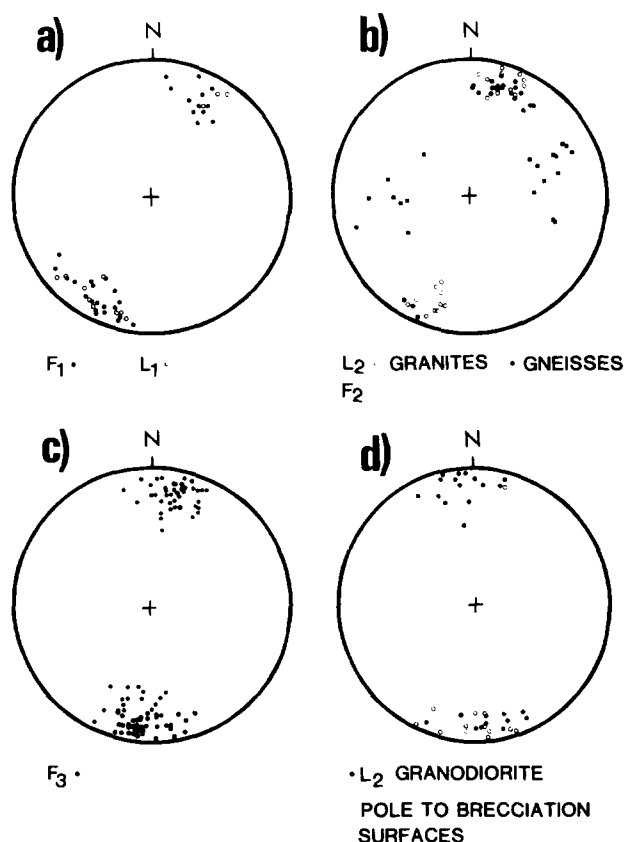


Fig. 4. Equal-area stereographic projections of: (a)  $F_1$  fold axes and  $L_1$  lineations; (b)  $F_2$  fold axes and  $L_2$  lineations; (c)  $F_3$  fold axes in meta-pelites and granites outside the leucogneiss core; (d)  $L_2$  lineations and the poles to sub-planar zones of chloritic brecciation in the post- $M_2$  granodiorite.

metric kinematic indicators in mylonitic fabrics. Transport directions implied by these indicators on Naxos are N to NE and S to SW (see below). For the sake of simplicity these will be described as northerly or southerly transport directions.

#### $D_1$ structures

$D_1$  structures are the earliest folds observed in the meta-pelite-dominated portion of the metamorphic complex. Large-scale  $F_1$  closures occur within the study area (Fig. 2, locality A). The structures developed are NNE-SSW-trending (Fig. 4a) asymmetric, isoclinal and often rootless similar-style folds (Figs. 5a, b & d). These folds have intense fold axis-parallel mineral elongation lineations ( $L_1$ ) (Figs. 4a and 6a). Axial-planar fabrics to  $F_1$  folds ( $S_1$ ) contain syntectonic amphibolite facies assemblages. On a meso-scale,  $F_1$  folds are usually cylindrical to mildly non-cylindrical. Less commonly highly non-cylindrical  $F_1$ (?) sheath folds have been observed in marbles (Fig. 5b). Fold limbs are invariably intensely boudinaged; boudin orientation and asymmetry generally indicates northwards-directed, sub-horizontal extension parallel to the fold axis. In general,  $F_1$  folds developed prior to the  $M_{2B}$  peak, since pelitic partial melt zones at the highest  $M_{2B}$  grades do not appear to be deformed by  $F_1$ .

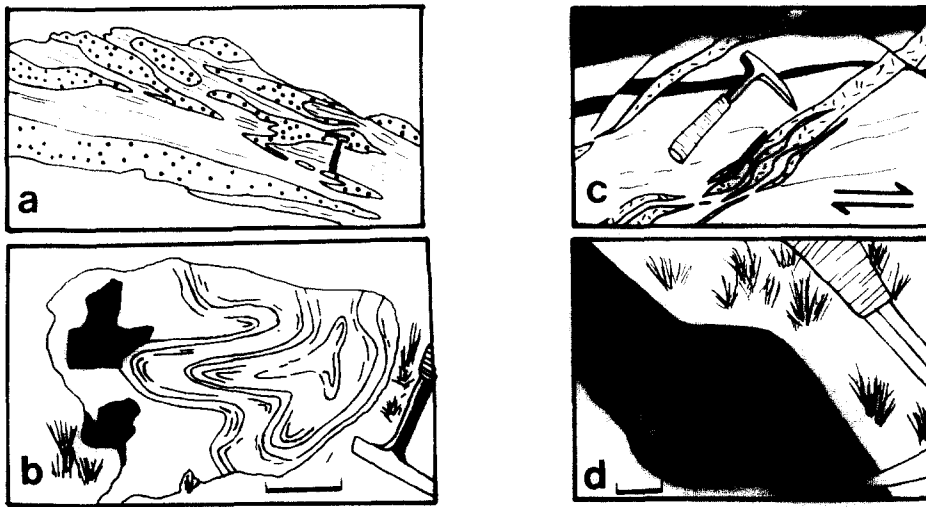


Fig. 5. Outcrop-scale structural relationships outside the leucogneiss core. All sketches are taken from field photographs. (a)  $F_1$  folds in an interlayered sequence of amphibolite facies meta-pelites and marbles (stippled), northwest of village of Apollonas (NE Naxos). (b) Sheath folds of possible  $D_1$  age in marble, Apeiranthos–Stavros road. Scale bar = 10 cm. (c)  $D_2$  asymmetric boudinage of biotite-granite dyke swarms within meta-psammitic gneisses. Boudin shear sense is dextral, and corresponds to top-to-the-north movement. 1 km south-west of locality D (Fig. 2). (d) Outcrop of black (graphitic) quartzite, showing  $F_1$  isoclinal folds in graphite-poor layers (stippled), re-folded by  $F_3$  folds with sub-vertical axial planes. Scale bar = 2 cm.

### $D_2$ structures

$D_2$  deformation is characterized by the development of protomylonitic to mylonitic fabrics ( $S_2$ ), and asymmetric boudinage (Figs. 5c and 6b) and folding.  $D_2$  structures also occur to a lesser extent in the underlying leucogneiss core. The effects of  $D_2$  deformation are most important in the northern half of the metamorphic complex.  $S_2$  mylonitic fabrics are sub-parallel to, and rework  $S_1$  fabrics in many lithologies. They invariably contain an intense NE–SW-trending stretching lineation ( $L_2$ ) (Fig. 4b). Composite  $S_{1/2}$  fabrics are frequently asymmetrically boudinaged (Fig. 6b), or deformed by small-scale, broadly E–W-trending tight folds ( $F_2$ ) (Fig. 4b) with gently inclined axial planes during continued  $D_2$  deformation. The ubiquitous occurrence of these highly asymmetric meso-structures indicates that  $D_2$  deformation was strongly non-coaxial. The sense of boudin and fold asymmetry indicates that upper structural levels moved to the north during  $D_2$ .

New  $S_2$  fabrics occur in post- $F_1$  biotite granites which intruded the meta-pelite-dominated sequence and the leucogneiss core during, or soon after, the  $M_{2B}$  peak (Jansen 1977). These granites intrude as dyke swarms, and in areas of low  $D_2$  strain are oriented at a high angle to the NE–SW elongation direction of the dome. This is particularly evident in the leucogneiss core. Granite dykes may be traced into domains of high resolved  $D_2$  shear strain, where they are rotated into sub-parallelism with the regional gneissic foliation. Within such higher strain zones, the intensity and distribution of  $S_2$  fabrics is heterogeneous, often on a scale of centimetres to metres. The larger intrusions are often less intensely, but more uniformly, deformed and are commonly protomylonitic  $L$  or  $L$ – $S$  tectonites. Intense, non-coaxial deformation of these large bodies is partitioned into 5–20 cm wide black mylonitic to ultramylo-

nitic shear zones. These steeply dipping ( $\sim 60$ – $70^\circ$ ), planar shear zones are sometimes truncated by weakly deformed pegmatites. The shear-sense obtained from dyke rotation, and asymmetric boudinage of small dykes (Fig. 5c) is consistent with that obtained from meta-pelites and indicates that upper structural levels moved to the north during  $D_2$ .

### $D_3$ structures

The structures formed during  $D_3$  deformation are upright, open to tight folds, essentially coaxial with  $F_1$  (Fig. 4c).  $F_3$  folds occur on mm to km scales and were the main structures mapped by Jansen (1973), and in this study (Fig. 2, localities A, B and C).  $F_3$  folds occur as broad regional antiform–synform pairs, with sub-vertical axial planes (Jansen 1973), but become moderately tight along the northwestern flank of the dome. The structural dome itself is an  $F_3$  anticline.

On the outcrop-scale,  $F_3$  folds are characterized by a fold axis-parallel crenulation lineation ( $L_3$ ), sometimes associated with a non-pervasive, sub-vertical spaced cleavage ( $S_3$ ).  $F_3$  meso-folds deform the composite  $S_1$ – $S_2$  foliation in the meta-pelite dominated sequences (Fig. 5d), and  $S_2$  fabrics in the granitic intrusives. The maximum difference in orientation between  $F_1$  and  $F_3$  folds in outcrop is usually  $<10^\circ$ .

## STRUCTURAL RELATIONSHIPS IN THE LEUCOGNEISS CORE

A similar structural history to that determined for the meta-pelite-dominated portion of the metamorphic complex can be observed in the leucogneiss core.  $D_1$ – $D_3$

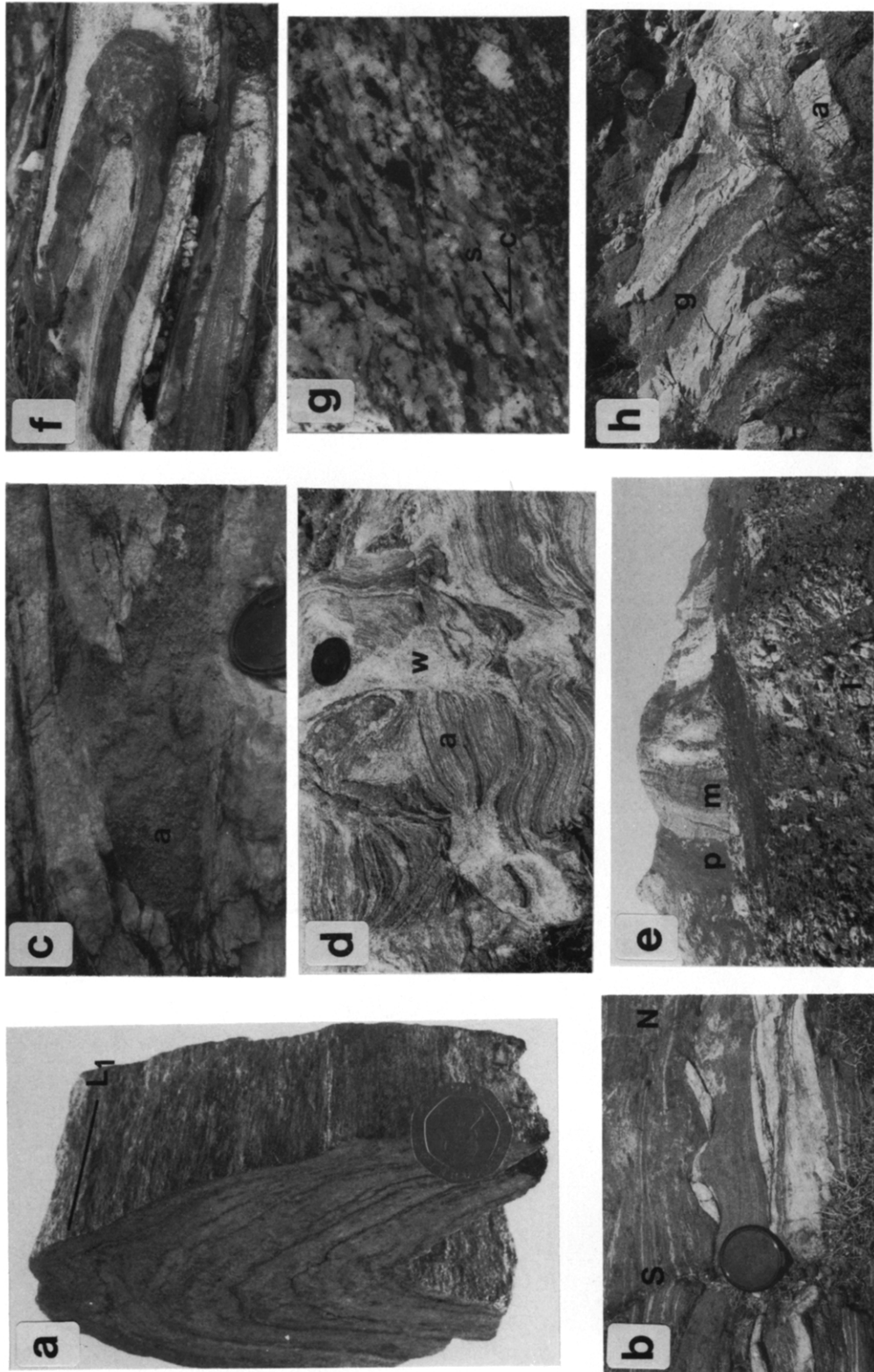


Fig. 6. (a)  $F_1$  meso-fold in quartzofeldspathic gneiss, showing intensely developed elongation lineation ( $L_1$ ), oriented parallel to the fold axis. (b)  $D_2$  asymmetric boudinage of aplitic interlayers within meta-psammites, western margin of the leucogneiss core. The dextral shear sense indicates top-to-the-north transport. (c) amphibolite xenolith (a) deformed by  $F_1$  fold in pre-peak  $M_{2B}$  granitic gneiss from the leucogneiss core. (d) Truncation of the foliation in pre-peak  $M_{2B}$  granitic augen gneisses (a) by syn- $M_{2B}$  wispy leucogneiss (w). (e) Discontinuous horizons of marble (m) and meta-pelite (p) within syn- $M_{2B}$  wispy leucogneiss (l). (f)  $F_1$  fold defined by amphibolite within a marble horizon, leucogneiss core. (g) Mylonitic  $S_2$  fabric in the post- $M_2$  granodiorite, western Naxos. The dextral asymmetry of S- and C-surfaces indicates top-to-the-north transport. (h) Upright, N-S-trending  $F_3$  fold defined by late applites (a) in weakly deformed post- $M_2$  granodiorite (g).

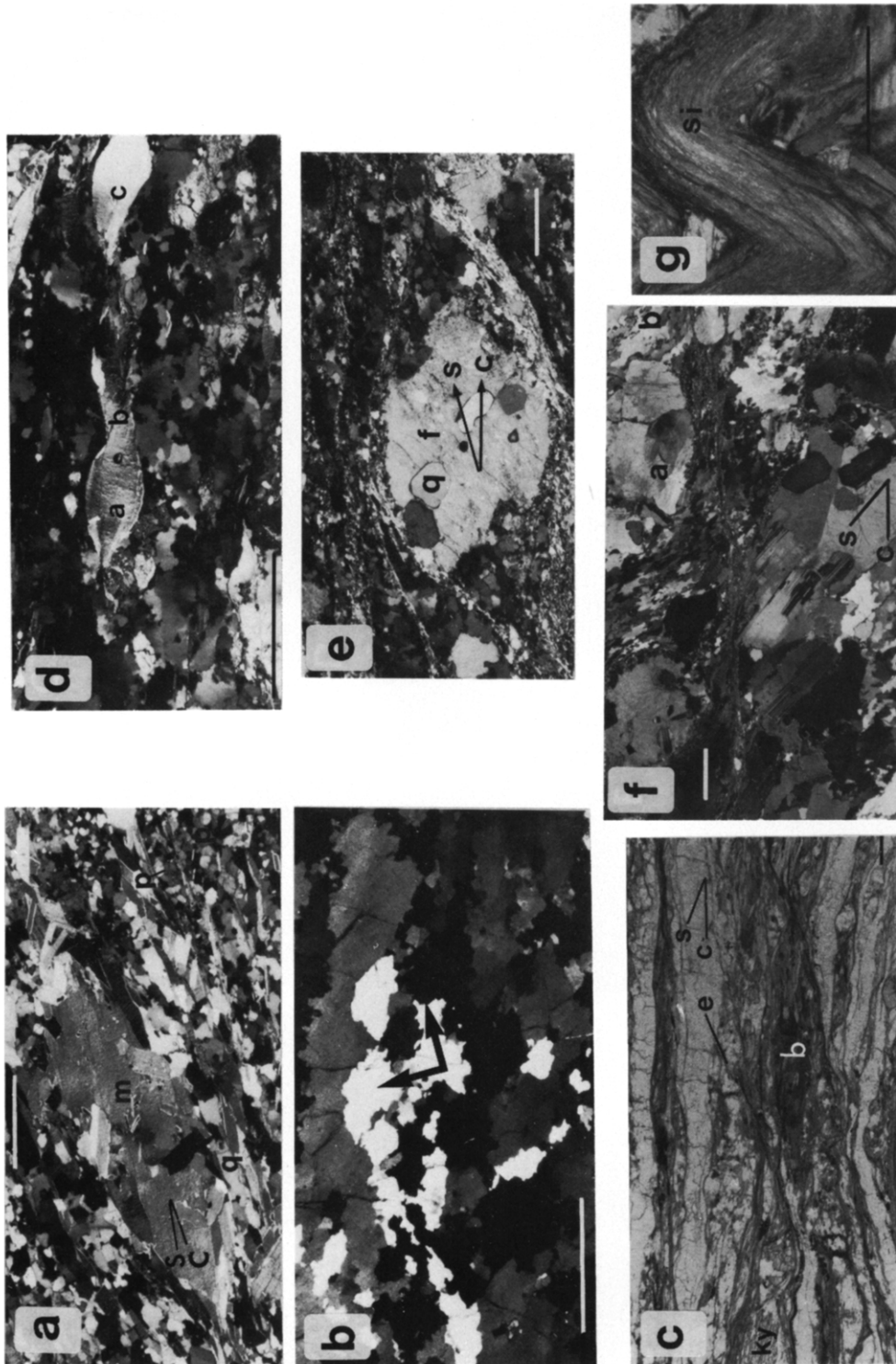


Fig. 7. Microstructures developed during  $D_1$ - $D_3$ . The asymmetry of kinematic indicators in (a), (c), (d) and (f) is consistent with transport of upper structural levels to the NNE. In all cases the scale bar = 1 mm. (a) Extensively recrystallized muscovite porphyroclast (m) within an aplitic layer deformed during  $D_1$ . Note the presence of an elongate, weakly deformed quartz ribbon (q), the fine-grained, annealed quartz-plagioclase mosaic (p), and the presence of S- and C-surfaces. Crossed polars. (b) High-temperature microstructures developed in quartz ribbons which define  $L_1$  in graphitic quartzites. Note the highly interpenetrative nature of grain boundaries and the conjugate nature of grain boundary alignments (arrowed). Crossed polars. (c) High-temperature  $S_2$  fabric in deformed meta-pelite. Kyanite (ky) remains stable in S-surfaces. S-C asymmetry is sinistral. S-C fabrics are cut by spaced shear band, or extensional crenulation cleavage zones (e); note retrogression of fabric biotite (b) adjacent to these cleavage zones. Plane polars. (d) Intermediate-temperature  $S_2$  mylonitic fabric in deformed migmatitic leucosome (northern margin of leucogneiss core). Sillimanite (not shown) is unstable in the S- and C-surfaces, being replaced by muscovite. Note internally deformed muscovite porphyroclasts (a and c), which show only minor recrystallization at grain boundaries. Micro-fault at (b) has opposite shear sense to sinistral bulk displacement. Crossed polars. (e) Mid-amphibolite facies  $S_2$  mylonite in a garnet-bearing granite dyke, NW Naxos. Note extensive recrystallization of quartz (q) and partial recrystallization of alkali feldspar (f) porphyroclasts. Crossed polars. Dextral shear sense. (f) Protomylonitic  $S_2$  fabric in the post- $M_2$  granodiorite, western Naxos. Note plastic deformation and recovery of feldspars (a) and variable recrystallization of quartz (b). Sinistral shear sense. Crossed polars. (g) Sillimanite (st) in amphibolite facies meta-pelite deformed by  $F_3$  micro-fold. Plane polars.

structures occur in a series of petrographically distinct, well foliated granitic gneisses (Figs. 2 and 6c). The  $S_1$  foliation in these granitic gneisses is truncated by poorly foliated, syn- $M_{2B}$  leucogranite ('wispy leucogneiss', Figs. 2 and 6d). Discontinuous marble horizons (Fig. 6e) also preserve evidence of  $D_1$  structures (Fig. 6f). Unambiguous  $F_1$  folds have not been observed in the wispy leucogneiss. Non-cylindrical, highly contorted folds do occur, but do not show consistent orientations or pervasive axial-planar fabrics. These folds have been suggested by Jansen & Schuiling (1976) to be flow folds.  $F_2$  and  $F_3$  meso-folds do, however, occur sporadically throughout the wispy leucogneiss.  $D_2$  deformation is less uniformly distributed in the leucogneiss core than in the overlying meta-sediments. It is characterized by narrow mylonitic to ultramylonitic shear zones in marble horizons and (less commonly) the wispy leucogneiss.  $D_2$  shear zones in marbles are planar and generally 5–30 cm in width. Calc-mylonite shear zones are oriented sub-parallel to the marble layering, and (rarely) exhibit NE–SW stretching lineations.

#### STRUCTURAL EVOLUTION OF THE POST- $M_2$ GRANODIORITE

The N–S-trending contact (Fig. 3) between the post- $M_2$  granodiorite and the metamorphic complex is intrusive in the southern, and tectonic in the northern halves of the island (Jansen & Schuiling 1976). Ductile deformation in the granodiorite is expressed by heterogeneous zones of  $D_2$  mylonites (Fig. 6g). The  $L_2$  lineation trends NNW–SSE to N–S (Fig. 4d) and is defined by stretched mineral aggregates and the preferred orientation of elongate quartz diorite xenoliths. The general northward increase in the intensity of  $D_2$  deformation, and the asymmetry of  $S$ – $C$  mylonitic fabrics (Fig. 6g) is consistent with the transport of higher structural levels to the north during  $D_2$ .

The granodiorite was also affected by  $D_3$  deformation. In regions of low  $D_2$  strain, contact aureole meta-pelites exhibit a weak  $L_2$  elongation lineation, defined by intergrown  $M_3$  andalusite and sillimanite. This lineation is sub-parallel to the hinges of  $F_3$  meso-folds which deform aplitic vein networks in the granodiorite (Fig. 6h). In high  $D_2$  strain zones, large-scale  $F_3$  closures in neighbouring marbles are tight to isoclinal in character (Jansen 1977), and are also oriented with hinge lines sub-parallel to the  $L_2$  stretching lineation.

The  $S_2$  fabric in the granodiorite is everywhere sub-parallel to the tectonic contact with the overlying unmetamorphosed tectonosedimentary unit. Retrogression and brecciation increase in intensity towards the contact with the tectonosedimentary unit, where ductile fabrics are almost completely obliterated, and pseudotachylites are developed (Jansen 1977).

#### MICROSTRUCTURAL DEVELOPMENT DURING DEFORMATION

##### $D_1$ microstructures

The microstructures developed parallel to  $L_1$  lineations in meta-pelitic, and other quartz-rich lithologies differ to some extent with geographic position in the metamorphic complex. In the southern half of the dome,  $S_1$  fabrics are often crystalloblastic. Microstructures are characterized by being weakly deformed or annealed, but highly elongate quartz ribbons, and a preferred, asymmetric orientation of porphyroblast phases such as kyanite occur in places.  $F_1$  micro-folds in profile also exhibit annealed microstructures and axial-planar mica fabrics. In quartzofeldspathic lithologies  $L_1$  lineations are commonly characterized by alternating quartz and plagioclase ribbons, pinned by mica porphyroclasts whose original shape has been extensively modified by recrystallization (Fig. 7a) (Lister & Snoke 1984). Plagioclase in this lineation is completely recrystallized to a fine grained, weakly elongated mosaic, often showing the development of  $120^\circ$  grain boundary junctions.

These annealed microstructures are interpreted as reflecting deformation at, or before the  $M_{2B}$  peak. This is consistent with the strong alignment of stable aluminous porphyroblasts or prograde reaction assemblages within the  $S_1$  fabric, and the less common occurrence of sigmoidal inclusion trails in porphyroblasts which indicate a top-to-the-north shear sense. The syn-tectonic nature of  $M_{2B}$  fabrics may be contrasted with the static nature of the  $M_{2A}$  greenschist facies overprint preserved at higher structural levels on Naxos (Urai in press), and on other islands in the Attic Cycladic Massif (Schliestedt *et al.* 1987).

In the central to northern portion of the metamorphic complex,  $L_1$  lineations are more commonly defined by quartz ribbons which show intense dynamic recrystallization (Fig. 7b). These lineations are statistically parallel to the hinges of  $F_1$  meso-folds that exhibit pervasive, dynamically recrystallized axial-planar fabrics. The quartz recrystallization microstructures, developed parallel to  $L_1$ , are characterized by an interpenetrative mosaic of relatively equant grains that often show conjugate grain-boundary alignments (Fig. 7b) (Lister & Dornsiepen 1982). These microstructures are interpreted as being the result of high-temperature grain-boundary migration (Lister & Snoke 1984, Urai *et al.* 1986). Oblique quartz foliations (Lister & Snoke 1984) often form useful kinematic indicators in these fabrics and consistently indicate a top-to-the-north shear sense. In the cases where conjugate grain-boundary alignments occur, shear sense from oblique foliations can not always be unambiguously determined. In these cases rare mica and plagioclase porphyroclasts usually indicate top-to-the-north shear. A subordinate component of dynamic recrystallization by progressive rotational misorientation of subgrains ('core and mantle structures', Poirier & Nicolas 1975) often accompanies grain-boundary

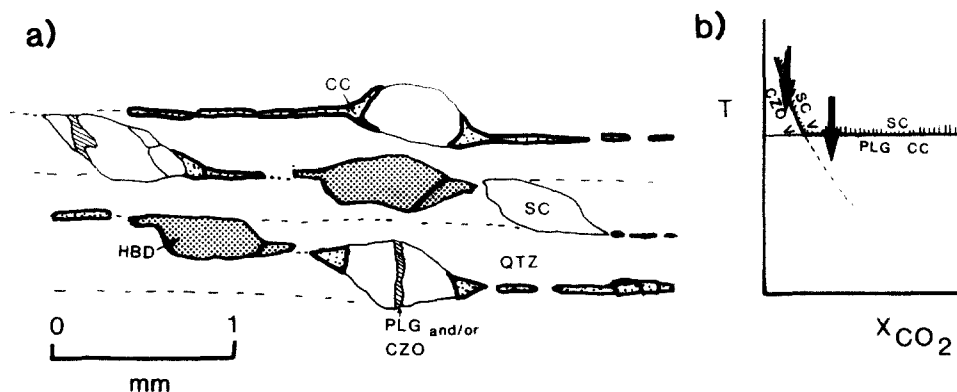


Fig. 8. (a) Sketch from a photomicrograph of mid-amphibolite facies mylonitized calc-silicate, showing augen of hornblende (HBD) and calcic scapolite (SC) within quartz (QTZ) ribbons. Scapolite shows incipient breakdown during  $D_2$  mylonitization to form calcite (CC) + plagioclase (PLG)  $\pm$  clinozoisite (CZO). (b) Inferred scapolite breakdown reactions calcic scapolite = calcite + calcic plagioclase and/or calcic scapolite +  $H_2O$  = clinozoisite +  $CO_2$  indicate cooling (arrowed) on isobaric T- $X_{CO_2}$  sections.

migration. This microstructure is common in impure quartzose gneisses, and becomes more common in overprinting fabrics developed at successively lower grades.

Where dynamic recrystallization microstructures are preserved, they record evidence of the last major strain increment during ductile deformation at, or after, the metamorphic peak (cf. Lister & Snoke 1984). These microstructures, observed in  $L_1$  lineations, can be used to approximately constrain metamorphic conditions during the last deformational imprint (cf. Lister & Dornsiepen 1982, Urai *et al.* 1986). Similar grain-boundary migration microstructures have been described by Wilson (1973), Kohlstedt & Weathers (1980), Bouchez & Pecher (1981), Lister & Dornsiepen (1982) and White (1982) from quartz-rich gneisses deformed under middle to upper amphibolite facies conditions. Conjugate grain boundary alignments in quartz aggregates are developed in most of these occurrences, and are thought by Lister & Dornsiepen (1982) to initiate at 600–700°C. This temperature range is comparable with that experienced during  $M_{2B}$  in the high-grade portion of the metamorphic complex. Likewise, extensive recrystallization of plagioclase in deformed quartzofeldspathic gneisses implies minimum temperatures >550–600°C, by analogy with both natural and experimental systems (White 1975, Tullis 1983, Jensen & Starkey 1985, White & Mawer 1988).

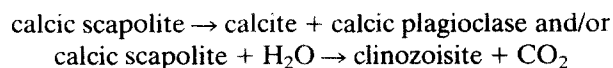
In view of these results, 550–600°C is considered to be a *minimum temperature* estimate for the development of microstructures preserved in  $L_1$  lineations. This compares with peak  $M_{2B}$  temperatures estimated from nearby meta-pelites of 600–670°C (Buick & Holland 1989). If the initial cooling of the highest-grade portion of the metamorphic complex, from peak  $M_{2B}$  conditions to ca 500°C, occurred as rapidly (1–4 Ma) as suggested by Wijbrans (1985), then the deformation responsible for these microstructures must also have occurred at, or soon after the  $M_{2B}$  peak.

#### $D_2$ microstructures

$S_2$  fabric evolution in the amphibolite facies portion of the metamorphic complex is typified by the sub-parallel

overprinting of higher, by lower, grade fabrics after the  $M_{2B}$  peak. With declining metamorphic grade high  $D_2$  shear strain was progressively partitioned into smaller rock volumes. Thus information about  $P$ – $T$  conditions during the development of sequential  $D_2$  structures is at least partially recoverable.

Initial  $D_2$  deformation in meta-pelitic lithologies produced Type II  $S$ – $C$  protomylonites and mylonites (Lister & Snoke 1984). These penetrative fabrics are characterized by the partial preservation of kyanite ( $S$ -surfaces) or fibrolitic sillimanite ( $S$ - and  $C$ -surfaces) and are inferred as having developed under amphibolite facies conditions (Fig. 7c). Within these fabrics, quartz grain aggregates typically exhibit a variable degree of dynamic recrystallization and mica porphyroclasts are often internally deformed (Fig. 7d). Similarly, in quartz-rich calc-silicates,  $D_2$  mylonitization began within the stability field of the amphibolite facies assemblage quartz, hornblende, clinopyroxene, calcic scapolite and grossular-rich garnet (Buick & Holland *in press*). In these calc-silicates, ubiquitous textural evidence of the reactions



in pull-aparts oriented at a high angle to the  $L_2$  lineation provides clear evidence of the retrograde nature of successive  $D_2$  fabric imprints (Fig. 8). In both meta-pelitic and quartz-rich calc-silicates the orientation of oblique quartz grain and subgrain fabrics, and asymmetric porphyroclasts consistently indicates that higher structural levels moved to the north during  $D_2$ . This conclusion is in agreement with meso-scale shear sense indicators.

In addition, the  $S_2$  foliation in meta-pelites is frequently deformed into lense-like packets by zones of non-pervasive 'shear band' (Cobbold *et al.* 1971) or 'extensional crenulation' (Platt 1984) cleavage. These cleavage zones make low (20–30°) angles with the trace of the main  $S_2$  foliation surfaces and cause N–S oriented, normal-sense offset across them (Fig. 7c). The microstructures developed adjacent to these zones include internal plastic deformation of porphyroclasts (feldspar,



muscovite, kyanite), chloritization of matrix biotite (Fig. 7c) and recovery or minor recrystallization of quartz. The cleavage zone fabric is usually defined by the greenschist facies assemblage quartz + muscovite  $\pm$  chlorite  $\pm$  haematite. Less commonly shear band fabrics are defined quartz + biotite. The asymmetry of these cleavage zones is not as reliable a kinematic indicator as asymmetric microstructures within the main  $S_2$  fabric; antithetic or conjugate shear band sets are not uncommon. Nevertheless, it is inferred that these zones of extensional, or shear band, cleavage represent a relatively late, non-penetrative  $S_2$  fabric imprint developed at lower grade than the main  $S_2$  mylonitic foliation.

Deformation in granitic intrusions within the high-grade core of the metamorphic complex is characterized by a wide range in the degree of deformation, recovery and recrystallization of quartz, plagioclase, alkali feldspar and micas. This variation is interpreted to primarily reflect differences in the grade of metamorphism attending deformation (cf. Simpson 1985), rather than differences in strain rate. This is because coeval fabrics developed in the surrounding gneisses, as described above, can be shown to have undergone fabric imprints defined by mineral assemblages formed at successively lower grade.  $S_2$  fabrics in biotite granite and garnet–two mica granite bodies near the margin of the leucogneiss core are characterized by extensive dynamic recrystallization of quartz, partial recrystallization of internally deformed mica porphyroclasts, and recovery and partial recrystallization of both plagioclase and microcline (Fig. 7e). This behaviour is generally consistent with deformation under middle amphibolite facies conditions (Simpson 1985). Asymmetric porphyroclasts within  $S_2$  imply a dominantly non-coaxial deformation with top-to-the-north shear sense, in agreement with meso-scale shear sense indicators.

$S_2$  fabrics in granitic bodies intruded at structural levels comparable with, or higher than, the sillimanite-in isograd of Jansen (1973) contain different microstructures. They are characterized by partially recrystallized quartz aggregates, low-temperature plasticity and minor recrystallization in both alkali and plagioclase feldspar, partial replacement of feldspars by muscovite  $\pm$  quartz in extensional fractures, and strong internal deformation of mica porphyroclasts. These microstructures are broadly indicative of deformation under lower amphibolite to upper greenschist facies conditions. Moreover,  $S_2$  fabrics developed under similar conditions sporadically throughout the leucogneiss core. This confirms that  $S_2$  fabrics formed over an extended time period, rather than simultaneously throughout the metamorphic complex at different grade, simply as a function of depth. Kinematic indicators within these  $S_2$  fabrics again usually indicate top-to-the-north movement.

$S_2$  fabrics in the post- $M_2$  granodiorite are extremely heterogeneous and within them deformation is governed by the crystal-plastic flow of quartz. Flattened quartz ribbons exhibit variable, but generally minor recrystallization, except in regions of localized strain

intensification around feldspar porphyroclasts (Fig. 7f). Quartz recrystallization occurs by progressive rotational misorientation of subgrains. Feldspars show evidence of low-temperature plasticity or have deformed by normal micro-faulting on surfaces oriented at a high angle to the  $L_2$  lineation. Biotite porphyroclasts are commonly kinked. These microstructures are consistent with  $D_2$  deformation under middle to upper greenschist facies conditions (cf. Simpson 1985). Greenschist facies deformation is also indicated by the widespread retrogression of igneous biotite, clinopyroxene, and hornblende to  $S_2$  fabric elements defined by aggregates of actinolite, calcite, epidote and chlorite. Once again, the resulting fabrics are highly asymmetric, and contain a wide range of kinematic indicators which indicate movement of upper structural levels to the north during  $D_2$ . These ductile fabrics are commonly overprinted by sub-vertical chlorite + calcite-rich normal-sense micro-fault or fracture systems, oriented sub-perpendicular to the  $L_2$  lineation (Fig. 4d).

### $D_3$ microstructures

$F_3$  micro-folds deform  $S_1$  and  $S_2$  without the development of a new pervasive axial-planar fabric. In metapelites these folds internally deform peak- $M_{2B}$  fibrolitic sillimanite (Fig. 7g) or kyanite, without recrystallization. Rarely, biotite and muscovite in  $F_3$  crenulation hinges show polygonized microstructures, suggestive of grain boundary adjustment at moderate metamorphic grade (e.g. in meta-pelites from the leucogneiss core). Where a spaced  $S_3$  crenulation cleavage is developed in meta-pelitic assemblages, it is defined by muscovite and (less commonly) biotite. This cleavage is interpreted as having grown under greenschist facies conditions. In upper structural levels, which experienced lower amphibolite peak- $M_{2B}$  conditions, it appears that the  $S_3$  cleavage developed simultaneously with greenschist facies mylonitic  $S_2$  fabrics, since both are defined by the same assemblages and contain similar deformation microstructures.

## DISCUSSION

### *Miocene ductile shearing on Naxos*

From the peak of the  $M_{2B}$  event (ca 19–20 Ma), until after the intrusion of the post- $M_2$  granodiorite (ca 13–11 Ma), gently dipping mylonitic fabrics ( $S_2$ ) developed on Naxos during conditions of progressively decreasing metamorphic grade. A consistent shear sense has been documented in this study from the majority of these non-coaxial fabrics. This kinematic co-ordination is interpreted as reflecting a continuum of sub-horizontal deformation with upper structural levels being transported to the north. The style and geometry of ductile deformation is consistent with the structures expected to develop in a major crustal shear zone, as suggested by Lister *et al.* (1984).

On Naxos, high-temperature deformation occurred rather uniformly throughout the *ca* 4 km thick succession of mylonitized amphibolite facies gneisses. Under lower temperature (though still relatively ductile) conditions, however, greenschist facies mylonites separate larger volumes of kinematically inactive, older high strain fabrics. The spaced greenschist facies  $S_2$  shear band cleavage, and the lack of evidence for rotation of  $F_2$  fold axes towards the bulk movement direction may reflect strain and rotational hardening and strain partition into more narrow zones with falling temperature during the latter stages of shear zone evolution (Platt 1983, 1984).

#### *Deformational setting*

The geometry of the ductile shear zone described on Naxos by itself gives no conclusive evidence as to the tectonic setting during deformation in the Cyclades (i.e. crustal compression or extension). Transport direction-parallel extension is a feature of non-coaxial deformation in both regimes. Evidence favouring an origin by crustal extension is somewhat indirect, and comes primarily from consideration of upper crustal normal faulting in the Aegean region. Sedimentary basins occur both to the north and south of the Attic Cycladic Massif. These basins indicate an extensional stress field for the Aegean from mid-Miocene times onwards (Le Pichon & Angelier 1979, Angelier *et al.* 1982). Similarly, the emplacement of unmetamorphosed sediments (i.e. tectonosedimentary units) onto metamorphic or granitic basement on Naxos and other Cycladic islands requires excision of several kilometres of intervening stratigraphy in the middle to late Miocene. This observation is most readily explained by low-angle, normal sense detachment faulting (Lister *et al.* 1984). On Mykonos and Delos (Faure & Bonneau 1988), and Naxos (Urai *in press*) the transport direction during emplacement of these tectonosedimentary units is the same as that determined from ductile mylonitic fabrics in the underlying metamorphic or granitic basement. Moreover, low-angle normal-sense faulting occurred on at least one Cycladic island (Tinos) contemporaneously with  $M_{2B}$  metamorphism on Naxos (Avigad & Garfunkel 1989).

Early ductile crustal excision also may have occurred across the leucogneiss core boundary on Naxos. This boundary must have represented a fundamental peak- $M_{2B}$  strain discontinuity, otherwise deformation would have been partitioned preferentially into the underlying partially melted granitic gneisses, at the expense of the unmelted overlying meta-pelite dominated sequence. The sense of displacement across this discontinuity is normal, since leucogneiss core meta-pelites experienced higher ( $P$ ,  $T$ ) conditions than those structurally overlying the leucogneiss core (Buick 1988, Buick & Holland 1989). Field evidence for a syn- $M_{2B}$  tectonic discontinuity of this kind occurs along the northwestern margin of the leucogneiss core, where protomylonitic high-grade gneisses, dipping at angles of 35–60° to the east,

are juxtaposed against the W-dipping boundary of the leucogneiss core (Fig. 2, locality D). This contact is thought to be tectonic in nature since the dip reversal does not appear to be the result of an  $F_3$  synformal closure. Since a large garnet–two mica granite dyke intrudes the contact without displacement (Fig. 2E), ductile faulting must have developed at, or near, peak- $M_{2B}$  conditions. Syn- $M_{2B}$  extension at this structural level has been suggested by Covey-Crump & Rutter (1989) to involve re-activation of pre- $M_1$  thrust surfaces.

Although syn- $M_1$ , N–S-trending isoclinal folds are preserved at low grade outside the study area (Bonneau *et al.* 1978, Hecht 1979) and on other Cycladic islands (e.g. Syros, Ridley 1986),  $F_1$  folds in the high-grade portion of the metamorphic complex are inferred to have developed during Miocene extensional shearing. This conclusion is based on the observation that  $D_1$  fabric elements are defined pervasively by  $M_2$  amphibolite assemblages or prograde reaction textures. In addition, less commonly, early  $M_2$  aplites are deformed by  $F_1$  folds. Recumbent structures of this type have been described from other extended terrains (e.g. Hodges *et al.* 1987, Malavielle 1987).

#### *Antithetic $S_2$ shear zones*

In a minority of samples studied, a top-to-the-SSE movement sense is implied by kinematic indicators in  $S_2$  mylonites. No consistent overprinting relationships between these fabrics and top-to-the-north  $S_2$  mylonites were observed.  $S_2$  mylonites with top-to-the-south asymmetry are interpreted as resulting from antithetic shear zones, subordinate to the bulk top-to-the-north transport direction. Such zones are a common feature of major crustal shear zones (Ramsay 1980, Lister & Snoke 1984). In one locality (Fig. 2, locality E), amphibolite facies  $S_2$  mylonites are developed along the margins of a series of garnet–two mica granites. These granites may be traced from the leucogneiss core, where they occur as undeformed, sub-vertical dykes, into the structurally overlying pelitic and semi-pelitic gneisses, where they are rotated into near-parallelism with the moderately dipping gneissic foliation. Along these dyke margins, the  $S_2$  fabric asymmetry indicates transport of upper levels to the south. This is in conflict with field relationships, which suggest top-to-the-north rotation of the dyke contacts into parallelism with the gneissic foliation. Lister & Snoke (1984) and Hodges *et al.* (1987) have described similar relationships, interpreted by Hodges *et al.* (1987) as resulting from layer-parallel shear, due to the greater competency of the deforming dykes as compared with the surrounding gneisses.

#### *Transport direction during Miocene extension*

The top-to-the-north shear sense determined throughout the exhumation history on Naxos disagrees with that described on Ios, and implied for Naxos, by Lister *et al.* (1984). A NE-directed shear sense has also been observed from mylonitic fabrics in middle Miocene

granitoids from the Cycladic islands of Mykonos and Delos (Faure & Bonneau 1988, Bonneau *et al.* 1989). If the exhumed metamorphic basement on Naxos, and other Cycladic islands does represent the deformed footwall of a large-scale, normal-sense shear zone (or a series of shear zones) then the distended and brittlely deformed hanging wall to this shear zone must occur to the north of the Cyclades, rather than in the Sea of Crete, as suggested by Lister *et al.* (1984). Miocene grabens of appropriate age and position occur to the north of the Cyclades, in the central and northern Aegean (Lachelos & Savoyat 1977, Le Pichon & Angelier 1979, Faure & Bonneau 1988). The significance of S-directed deformation on Ios (Lister *et al.* 1984) awaits further study.

#### *Significance of $F_3$ upright folding*

Open folds with hinges oriented parallel to mylonitic stretching lineations are a common phenomenon in shear zones (e.g. Nicolas & Boudier 1975, Hodges *et al.* 1987, Marcoux *et al.* 1987). On Naxos upright, open to tight  $F_3$  folds show such a relationship with respect to  $L_1$  and  $L_2$  stretching lineations. These folds deform all non-coaxial fabrics in the metamorphic complex and were developed after the  $M_{2B}$  peak under lower amphibolite to greenschist facies conditions. An open, N-plunging antiform with a similar orientation deforms the tectonic contact between the granodiorite and the tectonosedimentary unit (Fig. 3). Small-scale, NNW–SSE- to N–S-trending upright folds also occur in sediments within the tectonosedimentary unit.

The generally open nature of  $F_3$  folds requires that they nucleated in their present orientation, as any component of rotation into parallelism with the shear zone bulk movement direction would cause tightening and flattening of folds, and would result in isoclinal fold geometries (Cobbold & Quinquis 1980). It is interpreted that these folds reflect a component of E–W-directed sub-horizontal shortening during the later stages of N-directed ductile extension. East–west shortening in the Cyclades is consistent with geodynamic (Le Pichon & Angelier 1979) and paleomagnetic studies (Kissel & Laj 1988) of the Aegean, which indicate that the present-day angular shape of the Hellenic subduction zone is the result of deformation of an originally rectilinear, E–W-trending subduction zone by a combination of N–S extension and subordinate E–W compression. The rotation of the arc terminations accompanying this compressional component is thought to have occurred during two intervals. The first phase occurred during the middle Miocene (Le Pichon & Angelier 1979, Kissel & Laj 1988) and is interpreted to have produced the  $F_3$  folding observed on Naxos, and by implication other Cycladic islands. The second phase is Pliocene (*ca* 5 Ma) in age (Kissel & Laj 1988), and may have been responsible for the very late folding seen on Naxos after the emplacement of the tectonosedimentary unit in the interval *ca* 9–6 Ma (Roessler 1978, Andriessen *et al.* 1979).

## CONCLUSIONS

In this study the ductile deformation history on Naxos is interpreted as having occurred in a major normal-sense crustal shear zone. Models for the tectonic setting and driving force for this ductile extension are necessarily highly speculative. It is likely that Miocene extension in the Cyclades is related to a combination of internal body forces, generated during Eocene overthickening of the Aegean continental crust (Faure & Bonneau 1988), and tensional stresses, generated during oceanward retreat ('roll-back', Dewey 1980) of the Hellenic trench from the Miocene to its present-day position (Altherr *et al.* 1988, Dewey 1988, Wijbrans & McDougall 1988, Buick *in press*). Subduction zone roll-back is likely to be important for present-day extension in the Aegean. The relative contribution of catastrophic extensional collapse and plate boundary stresses throughout the Miocene extensional history of the Cyclades is, however, less clear and will not be speculated upon further.

The  $M_2$  isograd pattern on Naxos has traditionally been interpreted as a static thermal overprint on an earlier structural dome (Schuiling & Kreulen 1979). The results of this study, and that of Lister *et al.* (1984), disagree with this assertion, and emphasize the importance of syn- and post- $M_{2B}$  deformation in the metamorphic complex. The top-to-the-north movement sense ascribed to Miocene deformation on Naxos in this study is, however, opposite to that inferred by Lister *et al.* (1984). Ductile extension on Naxos was accompanied during its latter stages by a component of E–W-directed shortening. It is suggested that this shortening reflects rotation of the terminations of a Miocene subduction zone to the south of the Cyclades.

The syn- to post- $M_2$ , sub-horizontal ductile extension observed on Naxos implies a component of sub-vertical shortening, and should have resulted in a compressed sequence of  $M_{2A}$  and  $M_{2B}$  isograds. It is therefore unlikely that the present-day disposition and spacing of these isograds accurately reflects  $M_2$  conditions. Attempts to use  $M_{2A}$  and  $M_{2B}$  isograd spacing to calculate metamorphic field gradients (e.g. Jansen 1977, Wijbrans 1985) may need to be re-examined in the light of the Miocene extensional history of the metamorphic complex.

*Acknowledgements*—This paper represents part of the author's Ph.D. research in the Department of Earth Sciences, Cambridge, under the supervision of Tim Holland and Mike Bickle. Judy Baker, Barbara John, Mike Sandiford and Ron Berry are thanked for constructive criticism of earlier drafts of this manuscript. Reviews by Michel Bonneau and an anonymous referee greatly improved the final manuscript. Permission to undertake field work in Greece was given by IGME (Athens). Financial support from the University of Adelaide (George Murray Scholarship), the Gowrie Trust Fund, Overseas Research Scholarship Scheme and the Cambridge Commonwealth Trust Fund are also acknowledged. Cambridge Earth Sciences Contribution No. ES.1814.

## REFERENCES

- Altherr, R., Henjes-Kunst, F., Matthews, A., Friedrichsen, H. & Tauber hansen, B. 1988. O–Sr isotopic variations in Miocene

- Granitoids from the Aegean: evidence for an origin by combined assimilation and fractional crystallisation. *Contr. Miner. Petrol.* **100**, 528–541.
- Andriessen, P. A. M., Banga, G. & Hebeda, E. H. 1987. Isotopic age study of pre-Alpine rocks in the basal units on Naxos, Sikinos and Ios, Greek Cyclades. *Geologie Mijnb.* **66**, 3–14.
- Andriessen, P. A. M., Boelrijk, N. A. I. M., Hebeda, E. H., Priem, H. N. A., Verdurmen, E. A. Th. & Verschure, R. H. 1979. Dating the events of metamorphism and granitic magmatism in the Alpine Orogen at Naxos (Cyclades, Greece). *Contr. Miner. Petrol.* **69**, 215–225.
- Angelier, J., Lyberis, N. & Le Pichon, X. 1982. The tectonic development of the Hellenic Arc and the Sea of Crete: a synthesis. *Tectonophysics* **86**, 213–242.
- Avigad, D. & Garfunkel, Z. 1989. Low-angle faults above and below a blueschist belt—Tinos Island, Cyclades, Greece. *Terra Nova* **1**, 182–187.
- Bonneau, M., Faure, M., Pons, J. & Cottreau, N. 1989. Shear in Miocene granitic rocks of the northern Cyclades as a criterion for the determination of the sense of extension in the Aegean. *Abs. Vol., EUG V, Strasbourg*, 370.
- Bonneau, M., Geysant, J. & Lepvrier, C. 1978. Tectonique Alpine dans le massif d'Attique-Cyclades (Grèce): plis couchés kilométriques dans l'île de Naxos. Conséquences. *Rev. Géogr. phys. Géol. dyn.* **20**, 109–122.
- Bouchez, J.-L. & Pecher, A. 1981. The Himalayan Main Central Thrust Pile and its quartz-rich tectonites in Central Nepal. *Tectonophysics* **78**, 23–50.
- Buick, I. S. 1988. The metamorphic and structural evolution of the Barrovian overprint, Naxos, Cyclades, Greece. Unpublished Ph.D. thesis, University of Cambridge, U.K.
- Buick, I. S. In press. The Late-Alpine evolution of an extensional shear zone, Naxos, Greece. *J. geol. Soc. Lond.*
- Buick, I. S. & Holland, T. J. B. 1989. The *P–T–t* path associated with crustal extension, Naxos, Cyclades, Greece. In: *Evolution of Metamorphic Belts* (edited by Daly, J. S., Cliff, R. A. & Yardley, B. W. D.). *Spec. Publs geol. Soc. Lond.* **43**, 365–370.
- Buick, I. S. & Holland, T. J. B. In press. The nature and distribution of fluids during upper amphibolite facies metamorphism, Naxos (Greece). *J. metamorph. Geol.*
- Cobbold, P. R., Cosgrove, J. W. & Summers, J. M. 1971. The development of internal structures in deformed anisotropic rocks. *Tectonophysics* **12**, 23–53.
- Cobbold, P. R. & Quinquis, H. 1980. Development of sheath folds in shear regimes. *J. Struct. Geol.* **2**, 119–126.
- Coney, P. J. 1987. The regional tectonic setting and possible causes of Cenozoic extension in the North American Cordillera. In: *Continental Extensional Tectonics* (edited by Coward, M. P., Dewey, J. E. & Hancock, P. L.). *Spec. Publs geol. Soc. Lond.* **28**, 177–186.
- Covey-Crump, S. J. & Rutter, E. H. 1989. Thermally induced grain growth of calcite marbles on Naxos Island, Greece. *Contr. Miner. Petrol.* **101**, 69–86.
- Davis, G. H. 1980. Structural characteristics of metamorphic complexes. In: *Cordilleran Metamorphic Core Complexes* (edited by Crittenden, M. D., Jr). *J. geol. Soc. Am.* **153**, 79–129.
- Davis, G. H. 1987. A shear-zone model for the structural evolution of metamorphic core complexes in southeastern Arizona. In: *Continental Extensional Tectonics* (edited by Coward, M. P., Dewey, J. E. & Hancock, P. L.). *Spec. Publs geol. Soc. Lond.* **28**, 247–266.
- Davis, G. H. & Coney, P. J. 1979. Geological development of metamorphic core complexes. *Geology* **7**, 120–124.
- Dewey, J. F. 1980. Episodicity, sequence, and style at convergent plate boundaries. In: *The Continental Crust and its Mineral Deposits* (edited by Strangway, D. W.). *Spec. Pap. geol. Soc. Can.* **20**, 553–573.
- Dewey, J. F. 1988. Extensional collapse of orogens. *Tectonics* **7**, 1123–1139.
- Dürr, S., Altherr, R., Keller, J., Okrusch, M. & Seidel, E. 1978. The median Aegean crystalline belt: stratigraphy, structure, metamorphism, magmatism. In: *Alps, Appenines, Hellenides* (edited by Cloos, H., Roeder, D. & Schmidt, K.). Schweizerbart, Stuttgart, 455–476.
- England, P. C. 1987. Diffuse continental deformation: length scales, rates and metamorphic evolution. *Phil. Trans. R. Soc.* **A321**, 3–22.
- England, P. C. & Thompson, A. 1986. Some thermal and tectonic models for crustal melting in continental collisional zones. In: *Collisional Tectonics* (edited by Coward, M. P. & Ries, A. C.). *Spec. Publs geol. Soc. Lond.* **19**, 83–94.
- Faure, M. & Bonneau, M. 1988. Données nouvelles sur l'extension néogène de l'Égée: la déformation ductile du granite miocène de Mykonos (Cyclades, Grèce). *C.r. Acad. Sci., Paris Ser. II*, **307**, 1553–1559.
- Hecht, J. 1979. Geologische Karte des Schmirgel fuhrenden Gebietes zwischen Apiranthos und Koronos, Naxos-Griechenland; 1:10 000. Institute of Geology and Mineral Resources, Athens (Greek Legend).
- Henjes-Kunst, F. & Kreuzer, H. 1982. Isotopic dating of pre-Alpidic rocks from the island of Ios (Cyclades, Greece). *Contr. Miner. Petrol.* **80**, 245–253.
- Hodges, K. V., Walker, J. D. & Wernicke, B. P., 1987. Footwall structural evolution of the Tucki Mountain detachment system, Death Valley region, southeastern California. In: *Continental Extensional Tectonics* (edited by Coward, M. P., Dewey, J. E. & Hancock, P. L.). *Spec. Publs geol. Soc. Lond.* **28**, 393–408.
- Jackson, J. A. & McKenzie, D. 1983. The geometrical evolution of normal fault systems. *J. Struct. Geol.* **5**, 471–482.
- Jansen, J. B. H. 1973. The geology of Greece, Island of Naxos. Institute for Geology and Mineral Exploration (Athens).
- Jansen, J. B. H. 1977. Metamorphism on Naxos, Greece. Unpublished Ph.D. thesis, RU Utrecht, The Netherlands.
- Jansen, J. B. H. & Schuiling, R. D. 1976. Metamorphism on Naxos. Petrology and thermal gradients. *Am. J. Sci.* **276**, 1225–1253.
- Jensen, L. N. & Starkey, J. 1985. Plagioclase microfabrics in a ductile shear zone from the Jotun Nappe, Norway. *J. Struct. Geol.* **5**, 527–539.
- Kissel, C. & Laj, C. 1988. The Tertiary geodynamical evolution of the Aegean Arc: a paleomagnetic reconstruction. *Tectonophysics* **146**, 183–201.
- Kohlstedt, D. & Weathers, M. 1980. Deformation-induced microstructures, paleopiezometers and differential stresses in deeply eroded fault zones. *J. geophys. Res.* **85**, 6269–6285.
- Le Pichon, X. & Angelier, J. 1979. The Hellenic Arc and Trench system: a key to the neotectonic evolution of the eastern Mediterranean area. *Tectonophysics* **69**, 1–42.
- Lachelos, N. & Savoyat, E. 1977. La sédimentation néogène dans le fosse nord-égéen. *Sixth Colloquium on the Geology of the Aegean Region*, Athens, 6.
- Lister, G. S., Banga, G. & Feenstra, A. 1984. Metamorphic core complexes of Cordilleran type in the Cyclades, Aegean Sea, Greece. *Geology* **12**, 221–225.
- Lister, G. S. & Dornsiepen, U. F. 1982. Fabric transitions in the Saxony Granulite terrain. *J. Struct. Geol.* **4**, 81–92.
- Lister, G. S. & Snoke, A. W. 1984. S–C Mylonites. *J. Struct. Geol.* **6**, 617–638.
- Makris, J. 1978. The crust and upper mantle of the Aegean region from deep seismic soundings. *Tectonophysics* **46**, 269–284.
- Malavielle, J. 1987. Extensional shearing deformation and kilometer scale 'A'-type folds in a Cordilleran metamorphic core complex (Raft River Mountains, Northwestern Utah). *Tectonics* **6**, 423–448.
- Marcoux, J., Brun, J.-P., Burg, J.-P. & Ricou, L. E. 1987. Shear structures in anhydrite at the base of thrust sheets (Antalya, Southern Turkey). *J. Struct. Geol.* **9**, 555–561.
- McKenzie, D. 1978a. Active tectonics of the Alpine–Himalayan belt: the Aegean Sea and surrounding regions. *Geophys. J. R. astr. Soc.* **55**, 217–254.
- McKenzie, D. 1978b. Some remarks on the development of sedimentary basins. *Earth Planet. Sci. Lett.* **40**, 25–32.
- Nicolas, A. & Boudier, F. 1975. Kinematic interpretation of folds in Alpine-style peridotites. *Tectonophysics* **25**, 233–260.
- Platt, J. P. 1983. Progressive folding in ductile shear zones. *J. Struct. Geol.* **5**, 619–622.
- Platt, J. P. 1984. Secondary cleavages in ductile shear zones. *J. Struct. Geol.* **6**, 439–442.
- Poirier, J.-P. & Nicolas, A. 1975. Deformation-induced recrystallisation due to progressive misorientation of sub-grains, with special reference to mantle peridotites. *J. Geol.* **83**, 707–720.
- Ramsay, J. G. 1980. Shear zone geometry: a review. *J. Struct. Geol.* **3**, 83–99.
- Ridley, J. 1986. Parallel stretching lineations and fold axes oblique to a shear displacement direction—a model and observations. *J. Struct. Geol.* **8**, 647–653.
- Robertson, A. H. F. & Dixon, J. E. 1984. Introduction: geological evolution of the Eastern Mediterranean. In: *The Geological Evolution of the Eastern Mediterranean* (edited by Robertson, A. H. F. & Dixon, J. E.) *Spec. Publs geol. Soc. Lond.* **17**, 1–74.
- Roessler, G. 1978. Relics of non-metamorphic sediments on Central Aegean Islands. In: *Alps, Appenines, Hellenides* (edited by Cloos, H., Roeder, D. & Schmidt, K.). Schweizerbart, Stuttgart, 455–476.

- Sandiford, M. 1989. Horizontal structures in granulite terrains: a record of mountain building or mountain collapse? *Geology* **17**, 449–453.
- Schliestedt, M., Altherr, R. & Matthews, A. 1987. Evolution of the Cycladic Crystalline Complex: petrology, isotope geochemistry and geochronology. In: *Chemical Transport and Metasomatism* (edited by Helgeson, H. C. & Schuiling, R. D.). D. Reidel, Dordrecht. 76–94.
- Schuiling, R. D. & Kreulen, R. 1979. Are thermal domes heated by CO<sub>2</sub>-rich fluids from the mantle? *Earth Planet. Sci. Lett.* **43**, 298–302.
- Simpson, C. 1985. Deformation of granitic rocks across the brittle-ductile transition. *J. Struct. Geol.* **5**, 503–511.
- Sonder, L. J., England, P. C., Wernicke, B. P. & Christiansen, R. L. 1987. A physical model for Cenozoic extension of western North America. In: *Continental Extensional Tectonics* (edited by Coward, M. P., Dewey, J. E. & Hancock, P. L.). *Spec. Publs geol. Soc. Lond.* **28**, 187–201.
- Tullis, J. 1983. Deformation of feldspars. In: *Feldspar Mineralogy* (edited by Ribbe, P. H.). *Reviews in Mineralogy* **2**, 297–323.
- Urai, J. L. In press. Alpine deformation on Naxos (Greece). *Earth Planet. Sci. Lett.*
- Urai, J. L., Means, W. D. & Lister, G. S. 1986. Dynamic recrystallisation of minerals. In: *Mineral and Rock Deformation: Laboratory Studies—The Paterson Volume* (edited by Hobbs, B. E. & Heard, H. C.). *Am. Geophys. Un. Geophys. Monogr.* **36**, 161–199.
- Van der Maar, P. A. 1981. Metamorphism on Ios and the geological history of the Southern Cyclades. Unpublished Ph.D. thesis, RU Utrecht, The Netherlands.
- Van der Maar, P. A. & Jansen, J. B. H. 1983. The geology of the polymetamorphic complex of Ios, Cyclades, Greece and its significance for the Cycladic Massif. *Geol. Rdsch.* **72**, 283–299.
- Wernicke, B. & Burchfiel, B. C. 1982. Modes of extensional tectonics. *J. Struct. Geol.* **4**, 105–115.
- White, J. C. 1982. Quartz deformation and the recognition of recrystallisation regimes in the Flinton Group conglomerates, Ontario. *Can J. Earth Sci.* **19**, 81–93.
- White, J. C. & Mawer, C. K. 1988. Dynamic recrystallisation and associated exsolution in perthites: evidence of deep crustal thrusting. *J. geophys. Res.* **93**, 325–337.
- White, S. H. 1975. Tectonic deformation and recrystallisation of oligoclase. *Contr. Miner. Petrol.* **50**, 287–304.
- Wijbrans, J. R. 1985. Geochronology of metamorphic terrains by the <sup>40</sup>Ar–<sup>39</sup>Ar age spectrum method. Unpublished Ph.D. thesis, A.N.U., Canberra.
- Wijbrans, J. R. & McDougall, I. 1988. Metamorphic evolution of the Attic Cycladic Metamorphic Belt on Naxos (Cyclades, Greece) utilizing <sup>40</sup>Ar–<sup>39</sup>Ar age spectrum measurements. *J. metamorph. Geol.* **6**, 1–23.
- Wijbrans, J. R., Schliestedt, M. & York, D. 1990. Single grain argon laserprobe dating of phengites from the blueschist to greenschist transition on Sifnos (Cyclades, Greece). *Contr. Miner. Petrol.* **104**, 582–593.
- Wilson, C. J. L. 1973. The prograde microfabric in a deformed quartzite sequence, Mount Isa, Australia. *Tectonophysics* **19**, 39–81.